Notched-noise embedded frequency specific chirps for objective audiometry using auditory brainstem responses

Farah I. Corona-Strauss,[1,5] Bernhard Schick,[2] Wolfgang Delb,[1,3] Daniel J. Strauss[1,4,5]

[1]Systems Neuroscience and Neurotechnology Unit and [2]Department of Otorhinolaryngology, Saarland University Hospital, Homburg; [3]Department of Otorhinolaryngology, Mannheim University Hospital, Mannheim; [4]Leibniz Institute for New Materials, Saarbruecken, Germany; [5]Key Numerics Medical Engineering GbR, Saarbruecken, Germany

Abstract

It has been shown recently that chirp-evoked auditory brainstem responses (ABRs) show better performance than click stimulations, especially at low intensity levels. In this paper we present the development, test, and evaluation of a series of notched-noise embedded frequency specific chirps. ABRs were collected in healthy young control subjects using the developed stimuli. Results of the analysis of the corresponding ABRs using a time-scale phase synchronization stability (PSS) measure are also reported. The resultant wave V amplitude and latency measures showed a similar behavior as for values reported in literature. The PSS of frequency specific chirp-evoked ABRs reflected the presence of the wave V for all stimulation intensities. The scales that resulted in higher PSS are in line with previous findings, where ABRs evoked by broadband chirps were analyzed, and which stated that low frequency channels are better for the recognition and analysis of chirp-evoked ABRs. We conclude that the development and test of the series of notched-noise embedded frequency specific chirps allowed the assessment of frequency specific ABRs, showing an identifiable wave V for different intensity levels. Future work may include the development of a faster automatic recognition scheme for these frequency specific ABRs.

Correspondence: Farah I. Corona-Strauss, Systems Neuroscience & Neurotechnology Unit, Saarland University Hospital, Building 90.5 D–66421 Homburg/Saar, Germany.
Tel. + 49.6841.162.4091 - Fax: +49.6841.162.4092.
E–mail: corona@snn-unit.de

Key words: auditory brainstem responses, chirps, frequency-specific ABRs, single sweeps, phase synchronization, wavelet transform.

Conflict of interest: the authors report no conflicts of interest.

Received for publication: 23 September 2011.
Revision received: 5 January 2012.
Accepted for publication: 11 January 2012.

Audiology Research 2012; 2:e7
doi:10.4081/audiores.2012.e7

Introduction

The analysis of auditory brainstem responses (ABRs) is considered to be a robust method for the objective determination of hearing thresholds (HTs).[1,2] Such a method is of great relevance in the case of non-cooperative patients, i.e., newborns, in whom the application of behavioral methods is not possible, but where an early detection of a hearing loss and HTs and an opportune intervention and therapy are of great relevance, especially for the further development of the patients.[3,4]

The technical methods used to detect HTs in newborn hearing screening (NHS) programs include mostly transient evoked otoacoustic emissions (TEOAEs) and ABRs; other methods can also be employed, such as distortion product otoacoustic emissions (DPOAE).[5] TEOAEs can be used for a hearing check but they do not allow for a quantification of the hearing loss and suffer from a rather low specificity.[2] In general applications, *i.e.*, NHS programs, these methods give results related to a general HT, and when a more detailed frequency specific determination of a HT is required, *e.g.*, for hearing aid fitting, different approaches are used instead, *e.g.*, tone bursts-evoked ABRs, and auditory steady state responses (ASSRs).[6] The subjective methods used for the same purpose include pure tone audiograms (PTAs), but they still require the cooperation of the subject in order to perform the test. Lately, new methods such as the stacked ABRs,[7-12] which have been used for the detection of small acoustic tumors, seem to be a promising approach for frequency specific HT determination. The stacked ABR combines click-evoked ABRs with high pass filtered masking noise at different cutoff frequencies. The waves V for different frequency bands are determined by the subtraction of the averaged response obtained without masking condition (broadband response) to the averaged response using high pass filtered masking noise; then, the cutoff frequency of the noise is decreased for each subsequent measurement in order to extract the ABRs for the subsequent (lower) frequency bands.[7-12]

Over the last years it was commonly believed that ABRs were elicited by the onset or offset of a stimulus, and therefore clicks were preferred because of their abrupt onset and wide spectral content,[13,14] similar to the idea of a Dirac distribution activating all the Eigen values of a continuous linear time invariant system. However it is known that the cochlea is tonotopically organized.[15] This means that low frequency components of a traveling wave take a longer time to reach their sensation locus (apex) than the high frequency components (base), as shown in the schematic diagram of an uncoiled cochlea in Figure 1 (bottom). Gorga and Neely[16,17] reported wave V latency-intensity curves, where it can be seen that the latency and amplitude of the wave V of ABRs are related to the intensity and the frequency of the

stimulus. Later, Dau[18] designed a chirp stimulus with the idea of compensating the temporal dispersion of the basilar membrane (BM) by delaying the high frequency from the low frequency components, making use of the linear cochlear model of de Boer[15] and the cochlear frequency-position functions based on experimental data obtained by Greenwood,[19] see Figure 1 (top) for an example of a chirp stimulus. A variety of chirps have been developed since then. For instance, Fobel *et al.*[20] calculated chirps using otoacoustic emissions (OAE) data, and wave V-latencies fitted curves, they tested in control subjects and compared to the chirp developed by Dau *et al.*[18] and to click stimulations. Results showed larger wave V amplitude values using rising chirps compared to the amplitudes evoked by click stimulations. In particular, the chirps, which evoked the larger responses, were the ones based on the wave V latency-intensity curves. Chirp stimulations have not only been used for ABRs but also for auditory steady state responses (ASSRs)[21] and OAEs[22-24] applications, always resulting in positive results. For instance as reported by Elberling *et al.*,[21] the ASSRs evoked by chirps resulted in shorter detection time and higher signal-to-noise ratio compared to click stimulations. Likewise, Bennet *et al.*[22,23] employed chirp stimuli using the so called swept-tone technique to characterize the ear canal transfer properties and with this information an improved acoustical click could be developed and thus used to collect OAEs, resulting in a reduction of the stimulus artifact, a better signal-to-noise ratio also compared to a standard click stimulus, among other benefits. Also, Chertoff *et al.*[25] proved the advantage of using chirps instead of clicks for evoking the compound action potentials (CAPs). Specifically Wegner *et al.*,[26] generated a low-frequency chirp. The authors compared the resulting ABRs obtained with this low-frequency chirp and high pass filtered masking noise, to tone bursts-evoked ABRs, and concluded that the low frequency chirp-evoked larger wave V amplitudes at low and medium levels than a tone pulse with similar duration and magnitude spectrum. A series of band limited chirps was constructed by Bell *et al.*,[27] using the same approach reported by Dau *et al.*,[18] but without masking noise. Moreover, frequency windows to limit the bands of the chirps were employed. The authors obtained ABRs and concluded that the threshold estimations were similar to tone bursts stimuli without noise masking, but were different from the reported for tone burst using noise masking.

Due to a poor signal-to-noise ratio of ABRs, 2000 up to 4000 sweeps (individual responses) have to be often averaged to obtain a meaningful, visually noticeable signal at a particular stimulation level (the exact number depends on the number of artifacts produced and the stimulation intensity). This applies for ABR measurements including all its modalities (tone burst-evoked, stacked, notched noise-evoked ABRs, etc). This measurement time requires sometimes the state of spontaneous sleep, strong sedation, or narcosis of the newborns. Therefore, NHS programs are commonly conducted as multiple stage procedures, where the ABR measurements can just be applied at the last screening stage due to the long duration measurements. In other words, the idea is to filter as many as possible newborns by TEOAE measurements but due to a low specificity, many newborns with a physiological hearing are transferred to subsequent screening stages. This produces unnecessary cost due to the follow up. Therefore, a fast detection of frequency specific ABRs, and ABRs in general, would also be of great relevance and not only for click-evoked ABRs, where measurement is unsuitable in early screening stages of universal NHS programs.

So far, many methods have been proposed for an automatic recognition of ABRs with various success rates.[1,28-41] These methods are essentially based on traditional statistical pattern recognition techniques for classification of the ABRs. Generally, signal characteristics pertaining to different conditions are derived and then used for the computational recognition. Syntactic methods have also been used for the classification of ABRs.[32] Artificial neural networks have been used as well for

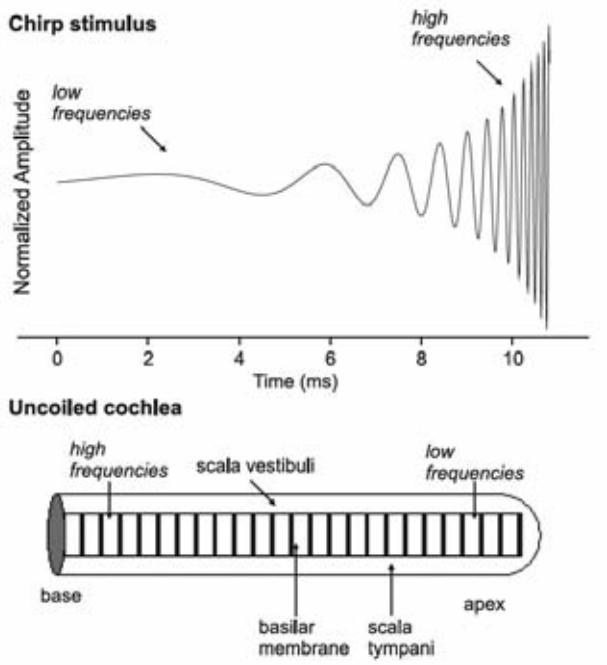

Figure 1. (Top) Chirp stimulus: Rising frequency chirp. Note that the high frequencies are delayed from the low frequencies. The amplitude envelope assures a flat amplitude spectrum. (Bottom) Schematic representation of an uncoiled cochlea. Note the tonotopic organization: the sensation loci for high frequencies are at the area of the base and for low frequencies are at the area of the apex.

classification of ABRs.[35] Chen *et al.*[37] reported a clinical evaluation of the widely used detection method ALGO, developed by Peters,[30] with a sensitivity of 93%, a specificity of 78% and an accuracy of 83%. Özdamar *et al.*[35] reported an accuracy of about 76% for ABRs classification by using back propagation multilayer perception classifier for the purpose of threshold determination. Gentiletti-Faenze *et al.*[40] reported a rather good sensitivity (91%), specificity (92%) and accuracy (91%) using an automatic ABR statistical recognition. Due to differences in the measurement techniques, data acquisition processes, and post-processing methods it is difficult to objectively compare the results of the research cited above. However, all these cited methods are based on large-scale averaging procedures for the final analysis and require sometimes narcosis, sedation, or the state of spontaneous sleep of the newborn to obtain the data. It is a major objective of our ongoing research to avoid time-domain averaging procedures, and instead use single sweep analysis in order to implement a very fast detection of ABRs, not only in terms of an acquisition of a general HT but also, for the detection of frequency specific responses as well.

The aim of the present work is to develop a series of frequency specific chirps, similar to the study of Bell *et al.*[27] but instead of symmetric frequency windows, using amplitude functions that result in flat spectrum chirps. Furthermore, the chirps will be embedded in notched filtered noise matching the frequency characteristics of each chirp. The latter will avoid synchronized contribution of other cochlear areas, *i.e.*, those areas that were not intended to be stimulated. Also, we showed recently that time-scale phase synchronization stability (PSS) provides a robust measure for the fast analysis of ABRs single sweep sequences.[42,43] The assessment of frequency specific ABRs could serve not only for HT determination but also for hearing aid fitting purposes, among other applications. In this paper we present the development of the notched-noise embedded band limited chirps, the resultant ABRs collected from healthy young subjects and their analysis using PSS.

This paper is organized as follows: in Materials and methods section

we present the construction of the series of notched-noise embedded band limited chirps, the experimental acquisition paradigm, subjects and measurement setup, as well as the post-processing methods applying the PSS measure to the collected ABRs. In Results and Discussion sections we present the findings and discuss our approach. Our conclusive remarks are finally given in Conclusions section.

Materials and methods

Stimuli

Chirps series

The generation of the chirps was based on the studies by Dau *et al*. and Fobel *et al.*,[18,20] where the latency-frequency function was developed employing the mathematical cochlear model of de Boer[15] and the cochlear frequency-position functions obtained by Greenwood.[19] First, a broadband chirp was calculated for the frequency range of 0.1-10 kHz (central frequency at 5250 Hz). This range of 9.9 kHz, which was the total operation range, served to generate the 5 bands (2^n, $n \in \{1, 2,..., 5\}$) for the frequency specific chirps. The bands were then centered on standard frequencies for audiograms (see theoretical values in Table 1). In ascending order, the smaller bands correspond to the low central frequencies and the larger bands correspond to the higher central frequencies, respectively. Next, an amplitude envelope which resulted in a flat frequency spectrum stimulus was applied,[18,20] combined with notched filtered masking noise. With the previously stated and ensuring that each stimulus started and ended with zero, it is presumed that the effect of an abrupt onset and offset of each stimulus is diminished. The chirps were adjusted to the latency-frequency function in order to have zero values at their beginning and at their end. For this series of chirps it was desirable to have as many cycles as possible in each stimulus. Thus, the duration criteria, besides the condition of 0 value at the beginning and at the end, was to have at least a minimum number of cycles. Wegner *et al*.[26] used a *3-half-waves* chirp, which we also took as criteria. The final bands of the chirps were slightly different from the first calculated bands (the frequencies changed less than 20%), and they remained under the tolerance limits according to the initial values (Table 1).

A special consideration was given to the chirps with the 2 highest frequency bands (Chirp number 4 and Chirp number 5). One chirp had to be constructed out of these two because the model did not allowed the *3-half-waves* criteria. Therefore, the ranges of both chirps were added and included in one chirp, resulting in 4 bands limited chirps. This limitation of the latency-frequency function and possible improvements will be discussed later in this paper. The final waveforms, as well as the latency-frequency function can be seen in Figure 2. In the same figure and in Table 1, the numerical values of the final central frequencies, frequency bands, and duration of the chirps are shown. For identification purpose, the chirps are called Ch1, Ch2, Ch3, and Ch4, according to their frequency range, where Ch1 accounts for the stimulus with the lowest frequency band and Ch4 refers to the chirp with the highest frequency band. For the broadband chirp the abbreviation is B-bCh. It is important to mention that the final chirps included the standard audiogram frequencies inside their range. The chirps were presented with an alternating polarity (one time the stimuli started with positive values and the next time with negative values) and a repetition rate of 20 Hz.

Notched masking noise

For the notched masking noise files, white noise as recommended in,[44] was created using scientific computing software (Mathworks Inc., USA). The noise was bandpass filtered for the frequency range of 0.1-10 kHz, afterwards it was notched filtered using digital finite impulse response filter. An individual notched-noise file was created for each chirp. The noise in all conditions was 20dB sound pressure level (SPL) smaller than the corresponding intensity of the chirps.[44] After calibration (for details see the subsection of calibration below), the noise was added to the stimuli and then presented to the subject. Note that the noise was not added to the broadband chirp as in this it was intended to stimulate the entire cochlea. All the stimuli were calculated digitally and converted to a sound file with a sampling frequency of 44.1 kHz.

Calibration

The setup and stimuli were calibrated according to the recognized standards and references,[45-47] *i.e.*, the peak equivalent (pe) SPL had to be calculated for the chirps. These peak amplitudes were measured

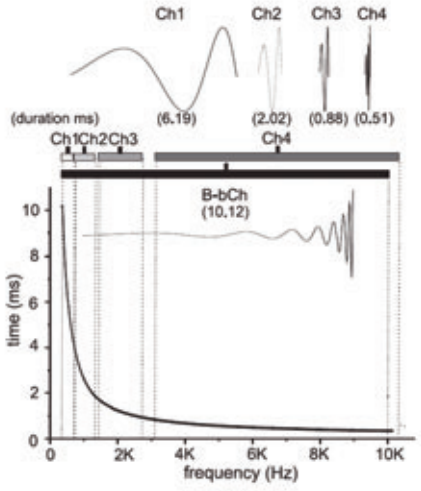

Figure 2. Frequency specific chirps. Thick black line: latency–frequency function used for the generation of the chirps. The resulting waveforms, frequency bands (displayed as horizontal bars), and duration of the chirps are also shown. Here, Ch1 corresponds to the chirp with the lowest frequency band and Ch4 corresponds to the chirp with the highest frequency band. B-bCh states for the broadband chirp.

Table 1. Calculated and final (') parameters of the frequency specific chirps. Note that the final Chirp 4 includes the ranges of Chirp number 4 and Chirp number 5, for details we refer to the text.

Chirp number	Bandwidth (Hz)	Fc (Hz)	Interval (Hz)	Fc' (Hz)	Interval' (Hz)	Duration (ms)
1	Range/2^5=309	250	[95, 405]	302	[108, 490]	6.1946
2	Range/2^4=619	750	[441, 1059]	813	[495, 1135]	2.0185
3	Range/2^3=1238	2000	[1381, 2619]	1915	[1230, 2600]	0.87806
4	Range/2^2=2475	4000	[2763, 5238]	6725	[2950, 10500]	0.5091
5	Range/2^1=4950	8000	[5525, 10475]	-	-	-
Broadband	Range/2^0=9900	5050	[100, 10000]	5050	[100, 10000]	10.12

from the highest peak to the most negative peaks using a digital oscilloscope (TPS 2014, Tektronix, USA), and the equivalent reference sinusoidal wave (to calculate the pe SPL) was produced by a function signal generator (33220A, Agilent, USA). A sound level meter (type 2250, Brüel & Kjær, Denmark) measured the pe SPL via a pre-polarized free field 1/2" microphone (type 4189, Brüel & Kjær) connected to an artificial ear (type 4153, Brüel & Kjær). The artificial ear was simultaneously coupled to the headphones (HDA-200, Sennheiser, Germany) while reproducing the reference sinusoidal wave. The noise files were calibrated by collecting their corresponding SPL values (Zeq) and subsequently were attenuated before adding them to their respective chirps.

Subjects, experiments, data preprocessing, and apparatus

Subjects

Chirp-evoked ABRs were collected from ten student volunteers of the Saarland University of Applied Sciences (mean age 25.1 years with a standard deviation of 3 years; 4 female, 6 male), with no history of hearing problems and normal hearing thresholds [below 15 dB (HL)] checked by an audiogram carried out before the experiments. After a detailed explanation of the procedure, all subjects signed a consent form.

Experiments and preprocessing

The time for one complete experiment was approximately 2 h including the time for the preparation of the subject and electrodes placement. Ag/AgCl electrodes (Schwarzer GmbH, Germany) were attached as follows: ipsilateral to the stimulus at the right mastoid (A1), common reference at the vertex (Cz), and ground at the upper forehead (Fpz). The electrode labels are according to the standard 10-20 system. Impedances were maintained below 5 kΩ in all the measurements. The subjects were instructed to lie down on a bed in an acoustically insulated room trying to remain quiet, with the eyes closed, and sleep if possible. The headphones were placed and after verifying electrode impedances, the lights were turned off. Subsequently, ABRs were obtained using the broadband chirp followed by the noise embedded frequency specific chirps for the intensity levels of 50, 40, and 30 dB pe SPL, respectively. In total 15 files were recorded. A total of 3000 sweeps, i.e., the response to an individual stimulus, free from amplitude artifacts (artifacts were removed by an amplitude threshold (15μV) detection) were recorded in each condition. The measurement sequence was identical for each subject.

Apparatus

Figure 3 shows the experimental set-up used for the acquisition of the ABRs. A personal computer controlled the acquisition of the electroencephalographic activity, as well as the presentation and intensity level of the stimuli. The electroencephalographic activity was acquired by a high-end 24 bit biosignal amplifier (gUSBamp, gTec, Austria) using a sampling frequency of 19.2 kHz, and a bandpass filter with low and high cutoff frequencies of 0.1 and 1.5 kHz, respectively. The biosignal amplifier was connected via USB port to the computer. The intensity level was controlled by means of a programmable attenuator headphone buffer (gPAH, gTec, Austria) connected to the computer via serial port. Each sound file was generated together with its respective trigger signal. The audio channel that corresponded to the stimuli was connected to the attenuator and afterwards delivered to the subject via circumaural headphones (HDA-200, Sennheiser). The trigger channel was connected to a trigger conditioner box (g.Trigbox, gTec) which adapted the voltage of the trigger signal in order to be acquired by the biosignal amplifier. The acquisition-processing program and all further post-processing were achieved using scientific computing software (Mathworks Inc., USA).

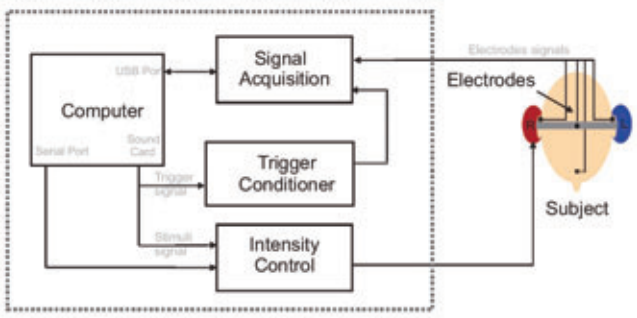

Figure 3. Set-up for the acquisition of auditory brainstem responses. The computer controls: (A) the acquisition of the electroencephalographic activity using a biosignal amplifier; (B) the intensity of the stimuli by using a programmable attenuator and headphone buffer; (C) stimuli and trigger signals presentation. The trigger signal is adequate for acquisition by a trigger conditioner box. The software developed for the specific purpose acquires, filters and stores the data.

Time-scale phase synchronization stability

In this section, we present the PSS derived from the complex continuous wavelet transform. Let $\psi_{a,b}(\cdot) = |a|^{-1/2}\ \psi((\cdot - b)/a)$ where $\psi \in L^2(\mathrm{R})$ is the wavelet with $0 < \int_{\mathrm{R}} |\Psi(\omega)|^2 |\Psi(\omega)|^{-1} d\omega < \infty$ ($\Psi(\omega)$ is the Fourier transform of the wavelet, and $a,b \in \mathrm{R}$, $a \neq 0$. The wavelet transform $W_\psi : L^2(\mathrm{R}) \rightarrow L^2(\mathrm{R}^2, \frac{da\,db}{a^2})$ of a signal $x \in \mathrm{L}^2(\mathrm{R})$ with respect to the wavelet ψ is given by the inner L^2-product $(W\psi x)(a,b) = \langle x, \psi_{a,b} \rangle_{\mathrm{L}}{}^2$. We define the PSS, $\Gamma_{a,b}$, of a sequence $\chi = \{x_m \in L^2(\mathrm{R}) : m = 1, \ldots, M\}$ of M sweeps by

$$\Gamma_{a,b}(\mathcal{X}) := \frac{1}{M} \left| \sum_{m=1}^{M} e^{\mathrm{i}\arg\left((\mathcal{W}_\psi x_m)(a,b)\right)} \right| \quad \text{Equation 1}$$

Note that Equation 1 yields a value in (0,1). For a more detailed explanation in the extraction of time-scale phase synchronization stability we refer to.[42,43,48] PSS of the collected ABRs was calculated using different values for the scale a. The pseudo-frequencies, F_a, can be calculated by $\frac{F_c \cdot F_s}{a}$ where Fc is the center frequency of the wavelet, and F_s is the sampling frequency.

Results

Auditory brainstem responses

Figure 4 shows an example of the ABR measurements in one subject for the different conditions. The results are shown in a single sweep matrix representation, *i.e.,* the amplitude of the sweeps is encoded in a color-scale map (yellow to white colors represent high values and dark red to black colors represent small values), and as thick black lines representing the averages for the time domain waveforms. Each line represents the average of the 1500 even and odd responses in order to show reproducibility. In the same figure the offset of the stimulus is subtracted in order to align the responses with the offset of their respective stimulus. The columns correspond to the responses for a specific intensity level (from left to right, 50, 40 and 30 dB pe SPL), and the rows from top to bottom, correspond to the responses of Ch4, Ch3, Ch2, Ch1, and B-bCh, respectively. The 6th row is the sum of the

responses from Ch1 to Ch4, and the last 7th row is the same sum but with prior alignment of the waves V. As mentioned in the previous section, 3000 sweeps were collected for each subject and condition. It is important to emphasize that we are interested in the feasibility to collect ABRs under the designed paradigm. In future, more clinical oriented applications, like for instance a fast detection of such ABR responses, the required number of sweeps to be collected would be much smaller, as observed in[49] in the range of hundreds, and factors such as the inter-stimulus interval (ISI) could also be decreased in order to optimize the data acquisition time.

The main results of the ABRs collected are summarized in Figure 5, where two separated plots to show mean latencies and mean amplitudes are shown. On the top of the Figure, the mean amplitude values of the wave V of ABRs are plotted for the different chirps and intensity levels. The plot at the bottom shows the latency-frequency function (black solid line-used for the generation of the chirps) as well as the resulting mean values of the latencies of the wave V of ABRs for the different chirps at the different intensity levels. Note that these averaged latency values are plotted in the center frequency of their corresponding chirp. In both figures, lines to connect the different averages are plotted for visual reasons; the black dot-dashed line, dark gray continuous line and light gray continuous line represent the results for intensities levels of 30, 40 and 50 dB pe SPL, respectively; the error bars represent standard deviation. The latency values for the B-bCh are shown as individual points at the center frequency of the broadband chirp. For the latency curves in this figure, the duration of the chirps is included and only 5 ms were subtracted from the preliminary average value. Those 5 ms represent the neural component[17] and it is not considered on the mathematical cochlear model, which is represented as a black thick line in the figure.

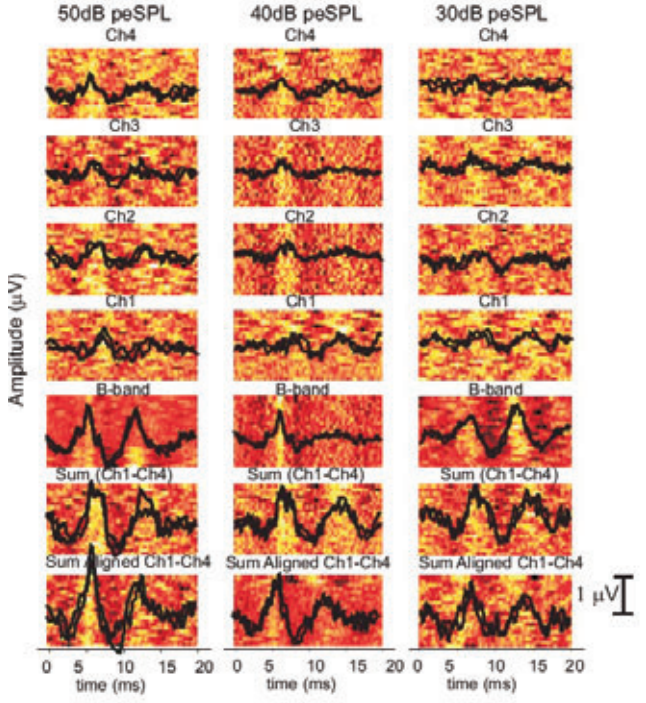

Figure 4. Example of auditory brainstem responses measurements collected from one subject for the different stimulation conditions. The columns correspond to the responses for a specific intensity level (from left to right, 50, 40 and 30 dB peak equivalent sound pressure level), and the rows (from top to bottom) correspond to the responses evoked by the Ch4, Ch3, Ch2, Ch1, and B–bCh, respectively. The row number 6 corresponds to the sum of the averaged responses of the Ch1, Ch2, Ch3, and Ch4, and the 7th row corresponds also to the same sum but after alignment of the waves V. For each condition, two black lines are plotted to show reproducibility (each line corresponds to an average of 1500 sweeps), and they are placed above its respective single sweep matrix representation, i.e., the amplitude of the sweeps is encoded in a color–scale map.

Time-scale phase synchronization stability

Figure 6 shows the grand average (overall the subjects) of the PSS for the different stimulation conditions, with M=3000 (sweeps), in Equation 1. For the calculations, the symmetric 6th-derivative of the complex Gaussian function was used as wavelet, and the value of the scale a ranged from 20 to 60 with increments of 5. The resultant center frequency Fc for this wavelet is 0.6 Hz. The organization of this figure (columns and rows according to intensity levels and chirp number) is the same as the one used in Figure 4. In Figure 6, red to black and yellow to white colors represent small and large values of PSS, respectively. The brighter color areas, *i.e.*, areas with high phase synchronization, are related to the presence of the wave V of ABRs and are easily extractable for middle to larger scales. In this figure, the duration times of the chirps were removed, as in Figure 4, in order to have the same time reference point, *i.e.*, the offset of the stimuli, and thus, facilitate comparison between measurements with Figure 4. Figure 7, shows the same PSS results of $\Gamma_{a,b}(X)$ but for the specific scale a=40, which was the scale that showed the best performance, i.e. higher values of $\Gamma_{a,b}(X)$ during the presence of wave V for the different stimulation conditions, which are specified on the same figure by gray arrows.

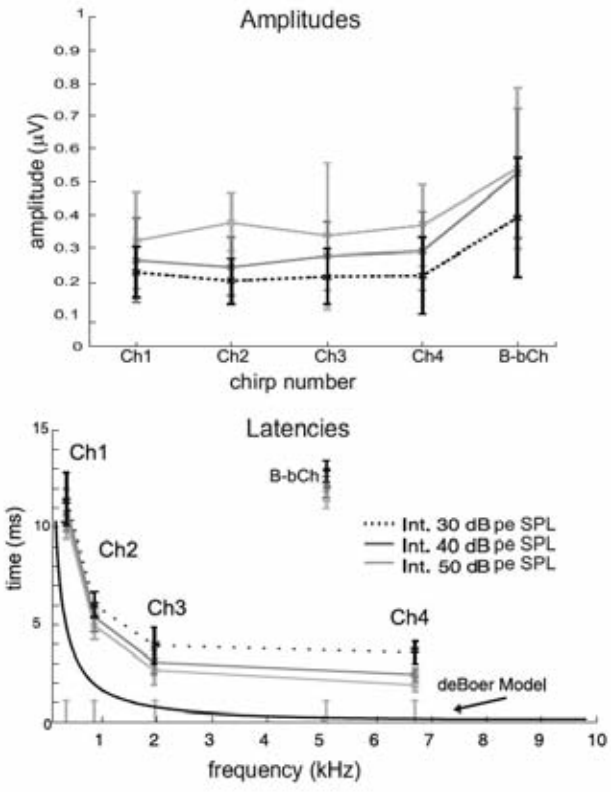

Figure 5. General auditory brainstem responses results. (Bottom) Wave V Latency curves: Average latencies obtained from all the subjects and for all stimulation conditions. The black continuous line represent the model of de Boer, employed in the generation of the chirps. (Top) Wave V mean amplitude values for the different stimulation conditions. In both figures: black dot–dashed line, dark gray continuous line, and light gray continuous line represent the intensity level of 30, 40 and 50 dB peak equivalent sound pressure level, respectively. The error bars indicate standard deviation.

Discussion

Chirp stimuli and auditory brainstem responses

The chirps, shown in Figure 2, were developed to stimulate specific areas along the cochlear partition. Therefore, and in order to avoid stimulation of undesired areas due to abrupt onset or offset stimulation, the chirps were calculated to start and end exactly with zero value. Also, in order to decrease synchronized activity from the rest of the cochlea, notched-noise was added to the stimuli. Moreover, the advantage of the flat amplitude spectrum windows is that they should stimulate all the fibers of the auditory nerve, which are of interest in the same proportion.

The study reported in[26] obtained ABRs responses with a similar paradigm like the one used in this work, but only one low frequency chirp (bandwidth of 100-480Hz) was tested and not a series that cover an important portion of the auditory range in humans. It could be argued that an alternative paradigm using a broadband chirp combined with noise could limit the response to the bands of interest. Nevertheless, the duration of all band limited chirps is much shorter than a broadband chirp, which would improve the acquisition time in applications where the obtention of a fast response is critical, such as frequency specific hearing threshold detection in newborns or during hearing aid fitting procedures. Anyway, after developing such a series of chirps, a comparison of both methods could be easily accomplished.

The trace of the wave V evoked by the different chirp stimulation is easily noticeable in Figure 4 from the color map representation and also from the averaged response (black lines). Note how the latency values increase as the frequency content of the chirps decreases. According to literature, these would be the expected results considering the tonotopic organization of the cochlea. Here high frequencies are delayed from low frequencies as a stimulus travels along the cochlea from the base to the apex. This effect is also clear in Figure 5 (bottom) where mean latencies of wave V of ABRs overall subjects are shown. It can be seen that in general, the latency values of ABRs responses evoked by chirps with high frequency content have shorter latencies as compared to the ones evoked by chirps with medium and lower frequency content, respectively. Also, it can be seen that latencies of responses evoked by higher intensity levels are in general shorter than softer intensity levels, which is also in accordance with existing literature, where latencies of wave V of ABRs evoked by tone bursts were normally employed.[13,16] The thick black line shows the mathematical cochlear model, developed by de-Boer, which was used to calculate the instantaneous phase function of the chirps, and is considered as a first order approximation of the behavior of the BM. Note that the mean latency values follow the same decreasing tendency as the model, but with the difference of an offset due to the intensity level employed to evoke the ABRs. The intensity variable is not included in the model, but a second generation of band limited chirps has been developed in parallel, using the wave V latency curves reported by Gorga and Neely.[16,17] Here the intensity factor is also included, but due to a simplification of the paradigm, and acquisition time, one series of chirps was tested first.

This second generation of chirps will be tested in future studies changing different variables in the paradigm as discussed later on this paper.

In the same Figure 5, the relation frequency-intensity of the stimuli and the latency of the wave V can be seen. For the highest intensity used in these experiments (50 dB pe SPL), the latencies are in general smaller as compared to the ones for lower intensities, such as 40 and 30 dB pe SPL. Likewise, the latency values for 40 dB pe SPL were smaller than the ones for 30 dB pe SPL. The latest was analyzed by an ANOVA test and the values which reached significance ($P<0.05$) were as follows: comparing intensity levels of 50 and 30 dB for the Ch2, Ch3, Ch4 and B-bCh; comparing intensity levels of 40 and 30 dB for the Ch3, Ch4 and B-bCh; and comparing intensity levels of 50 and 40 dB for the Ch4 and the B-bCh. In the same figure as well as in Figure 4 the larger latencies corresponding to the low frequency chirps stimulations (Ch1, Ch2) are noticeable, compared to the smaller latencies of the responses for higher frequency chirps (Ch3-Ch4). These results have the same behavior of the latency curves reported by Neely and Dau,[16,17] with the difference that instead of including a pure single frequency, they include a group of frequencies which covers a large percentage of the auditory range. The same is observed for latency results using

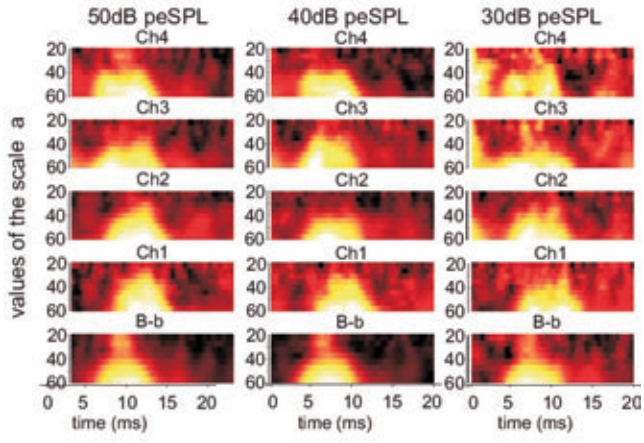

Figure 6. Grand average over all the subjects of $\Gamma a,b(X)$ (the scale a ranges from 20 to 60 with increments of 5), for the different stimulation conditions. The left, center and right columns correspond to the intensity levels of 50, 40 and 30 peak equivalent sound pressure level, respectively. The rows from top to bottom, correspond to the chirps Ch4, Ch3, Ch2, Ch1 and B–bCh, respectively.

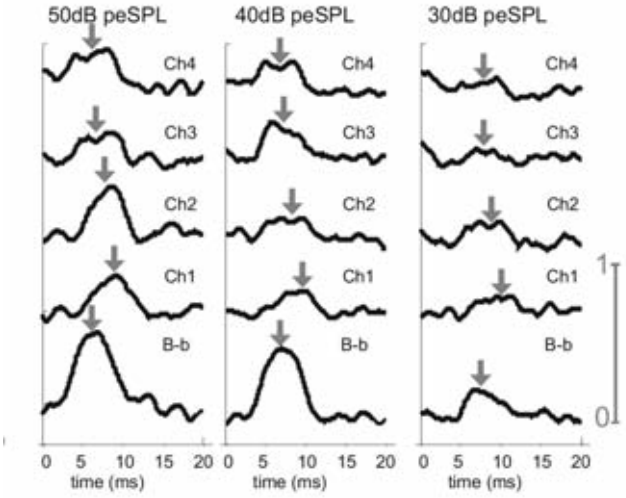

Figure 7. Grand average results of $\Gamma a,b(X)$ for the scale a=40. The left, center and right columns correspond to the intensity levels of 50, 40 and 30 peak equivalent sound pressure level, respectively. The rows from top to bottom, correspond to the chirps Ch4, Ch3, Ch2, Ch1 and B–bCh, respectively. The arrows indicate the mean latency of the wave V for the different conditions.

chirps.[26,50,27] The latency difference of the broadband chirps between the highest and lowest intensity level was 1.47±0.29 ms, and for the band limited chirps the latency difference was in the range of 1.98-2.56 ms for the lowest and the highest intensity level, respectively. The latency of the wave V is assumed to be a sum of a neural and a mechanical component.[17] The mechanical component is sensitive to frequency and intensity of a stimulus, while the neural component can be assumed as constant (5 ms).[17,21] Note that the latencies plotted in Figure 5 have a subtraction of 5 ms, which corresponds to such a neural component. This was done because the latency-frequency function, represented with a thick black line, includes only the mechanical properties of the BM.

The last rows 5-7 in Figure 4, correspond to broadband results. The 5th line, represents the results using the broadband chirp. The 6th row and the 7th are the result after adding the responses of the band limited chirps. The difference between these two waveforms is that for the 7th row, the averaged ABRs were first aligned with each other and then added. In general, all these waveforms show larger amplitudes compared to their individual band limited responses. This is also due to the fact that larger amount of the auditory nerve fibers were stimulated in a synchronous way using stimuli with a larger spectral content. The same can be observed in a general way overall the subjects on Figure 5 (top). There, it is easy to see that responses evoked by the B-bCh were larger in general compared to the amplitudes of the band limited chirps, the mean amplitudes evoked by the broadband chirps were 0.54, 0.52 and 0.39 μV for the intensity levels of 50, 40 and 30 dB pe SPL, respectively. On the other side, the amplitudes of the signals in the 7th row, in the Figure 4, are larger than the responses evoked by the broadband chirp and the summated response without pre-alignment (6th line). If a broadband chirp had an *ideal* instantaneous frequency function, i.e., the frequency components would be so perfectly organized such that each frequency would reach its sensation locus at the BM at the same time, a maximum response like the ones shown in the 7h row would be the result. This is difficult to accomplish in a general way, due to inter-subject variability. Nevertheless, a close to *ideal*, *i.e.*, generalized stimulus still can be developed and is the focus of ongoing research of different groups.[21,27] The 4th line on Figure 4 shows large latency values of the ABRs collected with the Ch1, the band limited chirp with the lowest frequency content. In order to increase the amplitude of the summated response on the 6th line, an extra adjustment of this low frequency chirp stimulus could be done. These changes could include, as it is also discussed later on this section, changes on the intensity level of the chirps which means that all of them could be adjusted and presented at the same sensation level as well as an adjustment of the intensity level of the masking noise for the different chirps.

On the other hand, when comparing amplitude values between intensity levels, it can be seen that all amplitude results for the different band limited chirps evoked at 50dB pe SPL intensity level, are larger than the corresponding responses evoked at 40 dB pe SPL, and the same follows for the 30 dB pe SPL responses when compared to 50 and 40 dB pe SPL. No particular amplitude tendencies were observed within band limited chirps at the same intensity level. The mean amplitudes were around 0.21 μV for the band limited chirps stimulations at 30 dB pe SPL, and 0.27 and 0.35 μV for the stimulation levels of 40 and 50 dB pe SP, respectively. In some studies reported in literature the chirp stimuli were presented using physiological measures of sound, *i.e.*, in dB sensation level (SL),[27,50] which required the determination of the individual hearing threshold for each type of stimulus. In order to avoid a subjective threshold adjustment every time when a different subject-stimulus combination was present, we obtained the pe SPL[45-47] for signals of short duration such as clicks and chirps. However, in order to have room for comparison, the 0 SL values were collected from all subjects. The normal Hearing Level (nHL) values of the chirps were calculated as the mean pe SPL of the detection threshold (0 dB SL) of the chirps at a repetition rate of 20 Hz. The resultant nHL values were: for Ch1 23.8±4.59 dB, for Ch2 21.5±4.62 dB, for Ch3 24.85±3.63 dB, for Ch4 36.93±3.99 dB, and B-bCh 31.5±3.61 dB. These values are similar to the ones found in literature. For instance the broadband chirp used by Dau *et al*.[50] had a mean pe SPL of 33.5±3.6 dB. In that study a broadband chirp similar to the one used in this work was used to evoke ABRs (referred as flat-spectrum chirp, with a bandwidth of 0.1-10.4 kHz). Their resultant mean amplitude values were approximately between 0.6 and 0.8 μV for the intensity levels ranging from 30 to 50 dB SL, these intensity levels are comparable to ours. Even so, the amplitude values from our measurements using the B-bCh were smaller, in particular oscillating between 0.4-0.55 μV. Wegner *et al.*[26] reported mean amplitude responses, collected with a low frequency chirp, of approximately 0.2 to 0.4 μV for intensity levels of 20 to 40 dB HL. The resultant amplitude values evoked by Ch1 were between 0.22 and 0.32 μV, for the lowest and highest intensity levels, respectively, which still within the aforementioned ranges. Nevertheless, a direct comparison with our results can not easily be done due to the fact that the 0 dB HL for their low frequency chirp was reported as 40 dB pe SPL, which differs from the 23.8 dB nHL of the low frequency chirp (Ch1) developed in this paper. The duration of both chirps was also similar, in the range of 6.5 ms, but the difference lies in the amplitude envelope, which is flat for Wegner *et al*.[26] and with a rising amplitude window for Ch1, i.e., the energy spectrum of both stimuli is different. In Bell *et al*.,[27] the band limited chirps had a 0 SL of 21, 24, 21 and 24 dB pe SPL, respectively for the low, medium, and high frequency chirps. These values are very similar to the nHLs of the chirps developed here, with a difference on the last high frequency chirp, which in our case has a broader spectral content. In the same publication, the amplitude values of the wave V were a little bit larger than what we found, in the range of 0.3 to 0.5. This could be due to the fact that in their paradigm no noise was present, thus a larger response could be expected.

Time-scale phase synchronization stability

In Corona-Strauss *et al.*,[42] the analysis of PSS was introduced for the robust analysis of single sweeps of chirp evoked ABRs, using broadband stimuli, i.e., broadband chirps and clicks. The idea of applying the same concept here was in order to find if the scale a of PSS to analyze frequency specific chirp-evoked ABRs might be different from the one for broadband chirps.

In Figure 6 it can be seen that, for all the conditions, the PSS is larger in the range of wave V. It becomes larger for the values of $a \geq 40$, where $a = 40$ corresponds to the frequency of 288 Hz. This is consistent to our previous findings,[42] where for Gabor frame phase stability (GFPS) analysis of chirp-evoked ABRs the channels with the highest energy of the ABRs corresponded to the frequency ranges of [160-230] and [320-480] Hz. In Figure 6, for the B-bCh, the PSS of the wave V is larger even for small values of a, which is supported by the fact that more fibers of the VIII-th nerve are stimulated. However, scale 40 still a good compromise between temporal and frequency resolution.

The areas of larger PSS represented with yellow and white colors, become broader for large values of a. This also implies a loss in temporal resolution. Note that the temporal resolution decreases as a increases. This is why it is relevant to find an optimal value, which results in a good compromise between temporal and frequency resolution, and again, a=40 seems to be a good supported choice given our limited amount of data. It can be concluded that the scale for the analysis of frequency specific chirp-evoked ABRs does not necessarily need to be different from the scale employed for broadband chirp-evoked ABRs. Consequently, the presented series of chirps can be used in our PSS scheme for the early HT detection in Corona-Strauss *et al.*[43] It is worthy to emphasize that PSS method allows for the analysis of single sweeps and can be used for the fast detection of ABRs. For instance, as

stated in Corona-Strauss *et al.*,[49] where with only 200 sweeps, the hybrid detection scheme allowed for a determination of a presence/absence of an ABR. Such a system for the fast detection of frequency specific ABRs can also be easily implemented.

The results presented in this paper are a first attempt to show feasibility of collecting ABRs using band limited chirps for different frequency bands. For this first attempt, some variables had to be fixed in order to simplify the paradigm and facilitate comparisons. For instance, the masking level used in this study, was 20 dB below the pe SPL of the stimulations, as recommended in the study by Stapells *et al.*[44] for low frequency specific brief tone bursts-evoked ABRs. It is also possible to analyze in further investigations which level of masking gives better results for low, medium and high frequency specific chirp stimulation. Another improvement, as previously stated in this paper, can be the use of chirps which include the intensity level factor as a parameter for their generation. Also, in this experiments, the chirps had always alternating polarity; this was done to avoid stimulus artifact. However, as mentioned by Gorga *et al*.,[51] the effect of the phase on the stimuli can also play an important role for the latency of the responses especially for low frequency stimulations. This effects can also be further investigated in future work.

A further step on the validation of this method includes a full comparison against established methods for frequency specific threshold determination, *e.g.*, tone bursts-evoked ABRs. An advantage of the band limited chirp-evoked ABRs is that they are not measuring the response of specific narrow areas of the cochlea, but instead of important fragments that include a wider but limited range of frequencies. All of these frequencies will contribute to the response in a more synchronize way, due to the physical characteristics of the chirps.

Conclusions

In this paper the development and test of a series of notched-noise embedded frequency specific chirps were described. The developed band limited chirps, allowed the assessment of frequency specific ABRs, with an identifiable wave V for different intensity levels. The resultant wave V latency measures showed a similar behavior as for the latency-frequency functions reported in literature. We conclude that we were able to extract frequency specific responses by means of the designed paradigm. The PSS of frequency specific chirp-evoked ABRs reflected the presence of the wave V for all stimulation intensities. The scales that resulted in a larger PSS are in line with previous findings, where ABRs evoked by broadband chirps were analyzed. This method can potentially be exploited for the fast recognition of frequency specific single sweep ABR responses using single sweep processing.

References

1. Wicke JD, Goff WR, Wallace JD, Allison T. On-line statistical detection of average evoked potentials: application to evoked response audiometry. Electroencephalogr Clin Neurophysiol 1978;44:328-43.
2. Delb W. Universal neonatal screening as an application of automated audiological techniques. HNO 2003;51:962-5.
3. Yoshinaga-Itano C. Benefits of early intervention for children with hearing loss. Otolaryngol Clin North Am 1999;32:1089-102.
4. de Aledo Linos AG. Programa de detection precoz de la hipoacusia infantil en Cantabria. Bol Pediatrics 2001;41:54-61.
5. Delb W, D'Amelio R, Schonecke O, Iro H. Are there psychological or audiological parameters determining the tinnitus impact. In: Hazell JWP, editor. Proceedings of the 6th tinnitus seminar. Cambridge, UK: Oxford University Press; 1999. pp. 446-451.
6. Luts H, Wouters J. Hearing assessment by recording multiple auditory steady-state responses: the influence of test duration. Int J Audiol 2004;43:471-8.
7. Eggermont JJ. Narrow-band AP latencies in normal and recruiting human ears. J Acoust Soc Am 1979;65:463-70.
8. Don M, Elberling C, Maloff E. Input and output compensation for the cochlear traveling wave delay in wide-band ABR recordings: implications for small acoustic tumor detection. J Acoust Soc Am 2009;20:99-108.
9. Don M, Eggermont JJ. Analysis of the click-evoked brainstem potentials in man unsing high-pass noise masking. J Acoust Soc Am 1978;63:1084-92.
10. Don M, Masuda A, Nelson R, Brackmann D. Successful detection of small acoustic tumors using the stacked derived-band auditory brain stem response amplitude. Am J Otol 1997;18:608-21.
11. Don M, Kwong B, Tanaka C, Brackmann DRN. The stacked ABR: a sensitive and specific tool fpr detecting small acoustic tumors. Audiol Neurotol 2005;10:271-90.
12. Elberling C, Don M. Auditory brainstem responses to a chirp stimulus designed from derived-band latencies in normal-hearing subjects. J Acoust Soc Am 2008;124:3022-37.
13. Hall JW. Handbook of auditory evoked responses. Needham Heights, MA: Allyn and Bacon; 1992.
14. Kodera K, Yamane, Yamada H, JI OS. The effect of onset, offset and rise-decay times of tone bursts on brain stem response. Scand Audiol 1977;6:205-10.
15. de Boer E. Auditory physics. Physical principles in hearing theory I. Phys Rep 1980;62:87-174.
16. Gorga PM, Kaminski JR, Beauchaine KA, Jesteadt W. Auditory brainstem responses to tone-bursts in normally hearing subjects. Speech Hear Res 1988;31:87-97.
17. Neely ST, Norton SJ, Gorga MP, Jesteadt W. Latency of auditory brain-stem responses and otoacustic emissions using tone-burst-stimuli. J Acoust Soc Am 1988;83:652-6.
18. Dau T, Wegner O, Mellert V, Kollmeier B. Auditory brainstem responses (ABR) with optimized chirp signals compensating basilar-membrane dispersion. J Acoust Soc Am 2000;107:1530-40.
19. Greenwood DD. A cochlear frequency-position function for several species-29 years later. J Acoust Soc Am 1990;87:2592-605.
20. Fobel O, Dau T. Searching for the optimal stimulus eliciting auditory brainstem responses in humans. J Acoust Soc Am 2004;116:2213-22.
21. Elberling C, Don M, Cebulla M, Stürzebecher E. Auditory steady-state responses to chirp stimuli based on cochlear traveling wave delay. J Acoust Soc Am 2007;122:2772-85.
22. Bennett CL, Ozdamar O. Swept-tone transient-evoked otoacoustic emissions. J Acoust Soc Am 2010;128:1833-44.
23. Bennett CL. Acquisition of otoacoustic emissions using swept-tone techniques. University of Miami; 2010.
24. Neumann J, Uppenkamp S, Kollmeier B. Chirp evoked otoacoustic emission. Hear Res 1994;79:17-25.
25. Chertoff M, Lichtenhan J, Willis M. Click-and chirp-evoked human compound action potentials. J Acoust Soc Am2010;127:2992-6.
26. Wegner O, Dau T. Frequency specificity of chirp-evoked auditory brainstem responses. J Acoust Soc Am 2002;111:1318-29.
27. Bell SL, Allen R, Lutman ME. An investigation of the use of band-limited chirp stimuli to obtain the auditory brainstem response. Int J Audiol 2002;41:271-8.
28. Woodworth W, Reisman S, Fointaine AB. The detection of auditory evoked responses using a matched filter. IEEE Trans Biomed Eng 1983;20:369-76.
29. Mason SM, Adams W. An automated microcomputer based electric

response audiometry system for machine scoring of auditory potentials. Clin Phys Physiol Meas 1984;5:219-22.
30. Peters JG. The ALGO-1: an automated infant hearing screener utilizing advanced evoked response technology. Hear J 1986;89:335-53.
31. Shangkai G, Loew MH. An autoregressive model of the BAEP signal for hearing threshold testing. IEEE Trans Biomed Eng 1986;33:560-5.
32. Madhavan GP, De Bruin H, Upton ARM, Jernigan ME. Classification of brainstem auditory evoked potentials by syntactic methods. Electroencephalogr Clin Neurophysiol 1986;65:289-96.
33. Delgado RE, Ozdamar O, Miskiel E. On-line system for automated auditory evoked response threshold determination. In: Proceedings of the 11th Silver Anniversary International Conference of the IEEE Engineering in Medicine and Biology Society; 1988. pp. 1472-1473.
34. Dobie RA, Wilson MJ. Analysis of auditory evoked potentials by magnitude-squared coherence. Ear Hear 1989;10:2-13.
35. Ozdamar O, Alpsan D. Neural network classifier for auditory evoked potentials. Adv Artif Int Res 1992;2:165-75.
36. Alpsan D, Towsey M, Ozdamar O, Tsoi A, Ghista GN. Determining hearing threshold from brain stem evoked potentials. IEEE Eng Med Biol Mag 1994;13:465-71.
37. Chen SJ, Yang EY, Kwan ML, Chang P, Shiao AS, Lien CF. Infant hearing screening with an automated auditory brainstem response screener and the auditory brainstem response. Acta Paediatr 1996;85:14-8.
38. Sanchez R, Riquenes A, Perez-Abal M. Automatic detection of auditory brainstem re-sponses using feature vectors. Int J Biomed Comput 1995;39:287-97.
39. Popescu M, Papadimitriou S, Karamitsos D, Bezerianos A. Adaptive denoising and multiscale detection of the V wave in brainstem auditory evoked responses. Audiol Neurootol 1999;4:38-50.
40. Vannier E, Adam O, Matsch JF. Objective detection of brainstem auditory evoked potentials with a priori information from higher presentation levels. Artif Int Med 2002;25:283-301.
41. Gentiletti-Faenze GG, Yanez-Suarez O, Cornejo JM. Evaluation of automatic identification algorithms for auditory brainstem response used in universal hearing loss screening. In: Proceedings of the 25th International Conference of the IEEE Engineering in Medicine and Biology Society. Cancun, Mexico; 2003. pp. 2857-2860.
42. Corona-Strauss FI, Delb W, Schick B, Strauss DJ. Phase Stability analysis of chirp evoked auditory brainstem responses by Gabor frame operators. IEEE Trans Neural Syst Rehabil Eng 2009;530-6.
43. Corona-Strauss FI, Delb W, Bloching M, Strauss DJ. Ultra-fast quantification of hearing loss by neural synchronization stabilities of auditory evoked brainstem activity. In: In Proceedings of the 29th Conference of the IEEE Engineering in Medicine and Biology Society. Lyon, France; 2007. pp. 2476-2479.
44. Stapells DR. Low-frequency hearing and the auditory brainstem response. Am J Audiol 1994;3:11-3.
45. European Committee for Standardization. Electroacustics-audiometric equipment. Part 3: test signals of short duration. The European Standard. EN 60645-3:2007; 2007.
46. International Organization for Standardization. Acoustics - Reference zero for the calibration of audiometric equipment. Part 6: Reference threshold of hearing for test signals of short duration. International Standards for Business. ISO 389-6:2007; 2007.
47. Richter U, Fedtke T. Reference zero for the calibration of audiometric equipment using clicks as test signals. Int J Audiol 2005;44:478-87.
48. Low YF, Corona-Strauss FI, Adam P, Strauss DJ. Extraction of auditory attention correlates in single sweeps of cortical potentials by maximum entropy paradigms and its application. In: Proceedings of the 3st International IEEE EMBS Conference on Neural Engineering. Kohala Coast, HI, USA; 2007. pp. 469-472.
49. Corona-Strauss FI, Delb W, Schick B, Strauss DJ. A Kernel-based novelty detection scheme for the ultra-fast detection of chirp evoked auditory brainstem responses. Conf Proc IEEE Eng Med Biol Soc 2010;2010:6833-6.
50. Dau T, Wegner O, Mellert V, Kollmeier B. Auditory brainstem responses with optimized chirp signals compensating basilar-membrane dispersion. J Acoust Soc Am 2000;107:1530-40.
51. Gorga PM, Kaminski JR, Beauchaine KL. Effects of stimulus phase on the latency of the auditory brainstem response. J Am Acad Audiol 1991;2:1-6.